

Thymosin α_1 Activates Complement Receptor-Mediated Phagocytosis in Human Monocyte-Derived Macrophages

Annalucia Serafino^a Francesca Pica^b Federica Andreola^a Roberta Gaziano^b
Noemi Moroni^a Gabriella Moroni^b Manuela Zonfrillo^a Pasquale Pierimarchi^a
Paola Sinibaldi-Vallebona^b Enrico Garaci^b

^aInstitute of Translational Pharmacology, National Research Council of Italy, and ^bDepartment of Experimental Medicine and Surgery, University of Rome 'Tor Vergata', Rome, Italy

Key Words

Complement receptor-mediated phagocytosis · Innate immunity · Macrophages · Phagocytosis · Thymosin α_1

Abstract

Thymosin α_1 (Ta1) is a naturally occurring thymic peptide used worldwide in clinical trials for the treatment of infectious diseases and cancer. The immunomodulatory activity of Ta1 on innate immunity effector cells has been extensively described, but its mechanism of action is not completely understood. We report that Ta1-exposed human monocyte-derived macrophages (MDMs) assume the typical activated morphology also exhibited by lipopolysaccharide-activated MDMs, but show a comparatively higher ability of internalizing fluorescent beads and zymosan particles. Ta1 exposure also promptly and dramatically stimulates MDM phagocytosis and killing of *Aspergillus niger* conidia starting as soon as 30 min after challenge. The effect is dose dependent and early coupled to low transcription of the proinflammatory cytokines tumor necrosis factor α and interleukin-6 and unmodified Toll-like receptor expression. The Ta1-stimulated phagocytosis is strictly dependent on the integrity of the microtubule network and protein kinase C activity and occurs

by a variation in the classic zipper model, with recruitment of vinculin and actin at the phagosome exhibiting a punctate distribution. These findings indicate that, in human mature MDMs, Ta1 implements pathogen internalization and killing via the stimulation of the complement receptor-mediated phagocytosis. Our observations document that Ta1 is an early and potent activator of innate immunity and reinforce the concept of its pleiotropy.

Copyright © 2013 S. Karger AG, Basel

Introduction

The monocytic/granulocytic system as well as differentiated macrophages constitute the primary cellular effectors of the immune response, playing a pivotal role in the detection and elimination of foreign bodies such as pathogenic microorganisms. Recognition of foreign microorganisms by these cells ultimately results in phagocytosis and destruction of pathogens by lysosomal enzymes. Macrophages perform a variety of functions other than phagocytosis [1]. The phagocytic process is accompanied by intracellular signals that trigger cellular responses such as cytoskeletal rearrangement, alterations in membrane

trafficking, activation of apoptosis and release of chemical mediators, i.e. growth factors, and pro- and anti-inflammatory cytokines and chemokines [2]. These mediators, which are produced by activated macrophages, are essential for microbe killing but also potentiate inflammatory reactions. The regulation of their production is therefore critical to killing pathogens without inducing tissue injury [3].

Thymosin α_1 (Ta1) is a naturally occurring thymic peptide first described and characterized by Goldstein et al. [4] in the 1970s. In the form of a synthetic 28-amino acid peptide [5, 6], Ta1 is included in clinical trials worldwide for the treatment of chronic hepatitis B and C [7–9] and cancer [10]. Additional indications are primary immune deficiencies [11], HIV/AIDS [7, 12] and impaired response to vaccination [13, 14].

Our group has provided an original contribution in defining the therapeutic potential of this peptide, with several preclinical studies aimed at evaluating the immune-modulating activity of Ta1 when used in combination with cytokines and/or chemotherapeutic drugs [10, 12, 15–18]. Evidence that Ta1, together with other immune stimuli, is capable of enhancing natural killer cell activity and inducing differentiation and maturation of T cells was first documented in our laboratory [15, 19]. In experimental animal studies performed in our laboratory, Ta1 was capable of protecting untreated or cyclophosphamide-pretreated recipient mice from intravenous challenge with *Candida albicans* at selected doses and schedules of administration [20]. This effect was associated with a significant augmentation in the number of circulating polymorphonuclear cells (PMNs) and of their candidacidal activity, although the issue of whether the effect of Ta1 on PMNs was a direct one on PMN precursor cells or mediated by other cell populations, such as lymphocytes or monocytes, remained unresolved at that time [21]. Studies by other groups of investigators also focused on the protective activity of Ta1 against opportunistic infections in animal models [22] and, more generally, on the capacity of Ta1 to potentiate several murine as well as human macrophage abilities [23–25]. Ta1 is able to upregulate the expression of the major histocompatibility complex class I in murine and human tumor cell lines and in primary cultures of human monocyte-enriched peripheral blood mononuclear cells (PBMCs) [26]. Ta1 can induce T-cell and dendritic cell (DC) maturation as well as interleukin (IL)-12 expression [27, 28]. In addition, Ta1 upregulates the expression of Toll-like receptors (TLRs) 2, 5, 8 and 9 in murine DCs and protects mice from challenge by invasive aspergillosis in the

MyD88 (myeloid differentiate factor 88)-dependent way [28]. Ta1 is capable of activating a TRAF6-atypical protein kinase C (PKC)-I κ B kinase signaling pathway that leads to the activation of nuclear factor- κ B, which in turn initiates cytokine gene expression in murine bone marrow-derived macrophages [29]. These studies provide relevant insights into how Ta1 exerts its immunomodulatory activity, but additional research is needed for a complete comprehension of the mechanism(s) involved in the Ta1-cell interaction.

The aim of the present study was to analyze the effect of Ta1 on the phagocytic and killing abilities of human monocyte-derived macrophages (MDMs) against different agents. The timing and modality of internalization and processing, and the involvement of phagocytosis-mediating cytoskeletal components were also examined.

Materials and Methods

Human MDM Cultures

PBMCs were isolated from buffy coats of healthy donors by density gradient centrifugation using lympholyte H (Cederlane, Hornby, Ont., Canada). The lymphocytic/monocytic fraction was then resuspended in RPMI 1640 medium (Hyclone, Logan, Utah, USA) supplemented with 10% (v/v) heat-inactivated fetal calf serum (FCS; Hyclone), L-glutamine (2 mM), penicillin (100 IU/ml) and streptomycin (100 mg/ml), and cells were seeded in 175-cm² flasks and maintained at 37°C in 5% CO₂ to obtain adhering MDMs. After 1 h of culture, nonadhering cells were removed and the residual adhering MDMs were maintained in culture for 7–10 days to obtain mature macrophages. Purity and maturation of macrophage cultures were tested by flow cytometry, analyzing physical (forward and side scattering) and immunological parameters (CD14, CD45 and CD44 expression; online suppl. fig. S1; for all online supplement material, see www.karger.com/doi/10.1159/000351587). Mature MDMs were then detached using cold phosphate-buffered saline, seeded at a density of 2.5×10^4 cells/cm² in 35-mm culture plates or on coverslips (\varnothing 10 mm) and allowed to adhere for 4–5 days before treatment.

Aspergillus Conidia Preparation and Staining

The *Aspergillus niger* used in this study was obtained from a clinical isolate and identified by conventional techniques. To exclude bacteria, the strain was grown on Sabouraud-chloramphenicol agar for 5 days at 37°C. Resting conidia were harvested by gently rinsing the plates with sterile 0.1% Tween 20 in saline, washed three times with distilled water, filtered through a sterile 100- μ m pore size nylon mesh (Falcon), resuspended in RPMI 1640 with 10% FCS at 1×10^9 /ml and stored at 4°C. Swollen conidia were obtained by shaking at 300 rpm for 8 h in RPMI 1640 with 10% FCS at 37°C.

For confocal microscopy, conidia were stained with Alexa Fluor 488 succinimidyl ester (Molecular Probes, Eugene, Oreg., USA) according to the manufacturer's instruction. This fluorescent probe selectively links to primary amines located on peptides and

proteins, also including those living on the cell surface. The excitation/emission wavelengths employed for the probe were 488/520 nm. After staining, conidial viability was tested evaluating their germination ability at 37°C for times ranging from 1 to 6 h (online suppl. fig. S2).

Treatment and Infection of Human MDMs

Ta1, a generous gift of Luigina Romani (Department of Experimental Medicine and Biochemical Sciences, University of Perugia, Perugia, Italy), was supplied as purified (the endotoxin levels were 0.03 pg/ml by a standard limulus lysate assay) sterile lyophilized acetylated polypeptide [28]. Human MDMs were treated for 1 h with Ta1 (50–100 ng/ml). MDMs stimulated with 0.2 µg/ml of bacterial lipopolysaccharide (LPS, Sigma-Aldrich, St. Louis, Mo., USA) for the same time were used as a positive control of macrophage activation. For analysis of MDM-conidia interaction, human macrophages were exposed to 100 ng/ml Ta1 for 1 h and subsequently incubated at 37°C with *A. niger* conidia (about 10 conidia/cell) for additional times ranging from 30 min to 24 h. For optical, confocal and scanning electron microscopic (SEM) analyses, cells were grown on coverslips as indicated above.

Optical Microscopy, Scanning and Transmission Electron Microscopy

Analyses of the morphological features shared by activated MDMs were carried out by phase-contrast microscopy after Wright-Giemsa staining and by SEM. The ultrastructural study of *A. niger* conidial internalization was elucidated by transmission electron microscopy (TEM). For SEM, MDMs were processed as described previously [30] and detailed in the supplementary Materials and Methods. Quantitative assessment of the number of adhering conidia on the cell surface was performed 30 min after challenge by analyzing a minimum of 100 cells per sample; results were expressed as mean values of three different experiments.

For TEM, treated and untreated cells were fixed for 2 h with 2.5% glutaraldehyde in 0.1 M Millonig's phosphate buffer containing 2% sucrose and then postfixed for 8 h with 1% OsO₄ in the same buffer. Samples were then dehydrated in ascending acetone concentrations and embedded in Spurr epoxy resin (Agar Scientific, Stansted, UK). Semithin sections of cells were stained with methylene blue (Sigma-Aldrich). Ultrathin sections were stained with uranyl acetate and lead citrate and observed under a Philips CM12 transmission electron microscope (Philips, Eindhoven, The Netherlands) operating at 80 kV.

Evaluation of the Phagocytic Activity of Human MDMs

The phagocytic activity of treated and untreated MDMs was tested by confocal laser scanning microscopy (CLSM) or by TEM, using the following methods:

(1) by adding to the cultures 2×10^7 beads/ml of yellow-green fluorescent polystyrene beads (\varnothing 1 µm, at a ratio of at least 10 beads/cell; Molecular Probes) as previously described [30] and detailed in the online supplementary Materials and Methods. A minimum of 200 cells per sample was observed by confocal microscopy, and the number of phagocytic MDMs (reported as percent of phagocytic cells), as well as the number of beads per cell, were counted;

(2) by evaluating under a confocal microscope the ingestion of fluorescent zymosan A BioParticles (Molecular Probes) covalently labeled with Alexa Fluor 594 (Abs/Em: 590/617, red fluorescence).

Zymosan particles were added to the culture medium at a ratio of 20 particles/cell. After 2.5 h, cells were fixed with 4% paraformaldehyde and counterstained with 0.2% Hoechst (Sigma-Aldrich) for nucleus visualization. The number of internalized zymosan particles per cell was evaluated by analyzing a minimum of 200 cells for each sample;

(3) by TEM analysis performed on thin sections from resin-embedded cells 2.5 h after challenge with *A. niger* conidia. The percentage of phagocytic cells and the number of ingested conidia were calculated on sequential sections by examining a minimum of 50 cells per sample.

For the quantitative assessment performed according to the techniques described in (1) and (2), each experiment was repeated at least three times, and mean values were plotted. At least 10 buffy coats from different healthy donors were analyzed.

Evaluation of the Ability of MDM to Process and Disassemble A. niger Conidia

Quantitative assessment was carried out by CLSM after staining of lysosomes and proteolytically active intracellular compartments with the specific fluorescent probes LysoTracker-Red and DQ-BSA-Red (Molecular Probes), respectively. MDMs pretreated with Ta1 (100 ng/ml for 1 h) and untreated controls were challenged with *A. niger* conidia, loaded with 75 nM LysoTracker-Red or 10 µg/ml DQ-BSA-Red probes 5 h after challenge, and fixed with 4% paraformaldehyde 1 h later. The effect on fungicidal activity was then evaluated 6 h after challenge and after an additional 18 h of culture in conidium-free medium (24 h after challenge) by CLSM. The merged images of differential interference contrast (DIC), used for visualizing cells and conidia, and LysoTracker or DQ-BSA fluorescence were assessed. The percentage of internalized conidia colocalizing with both lysosomal and proteolytically active intracellular compartments were calculated by analyzing a minimum of 200 cells per sample.

Quantitative Reverse Transcription Polymerase Chain Reaction

The effect of treatments on gene transcription was evaluated by quantitative polymerase chain reaction (qPCR) in untreated controls and MDMs pretreated for 1 h with Ta1 (100 ng/ml) or LPS (0.2 µg/ml), before and after a 30-min and 1-hour challenge with *A. niger* conidia. Total RNA extraction and qPCR were performed as reported previously [30] and detailed in the online supplementary Materials and Methods. The sequences of primers used in the assays are reported in online supplementary table 1.

Evaluation of Cytokine Release

The concentration of proinflammatory and immune-modulating cytokines (TNF-α, IL-1β, IL-4, IL-6, IL-10 and IL-12p70) released into the culture media by Ta1-treated MDMs were determined using the BD cytometric bead array human inflammation flex set (BD Pharmingen, San Diego, Calif., USA) according to the manufacturer's protocol [31, 32]. The threshold of the sensitivity of the assay in our hands ranged from 5 to 10 pg/ml for all cytokines tested, as demonstrated by the respective standard curves. Cytokine release by MDMs was tested before and 30 min or 1 h after the *A. niger* conidial challenge. Flow-cytometric analysis was carried out using a FACSCalibur flow cytometer (Becton Dickinson, Mountain View, Calif., USA). As a control, the effect of LPS on the same parameters was also evaluated.

Inhibition Experiments

Treated and untreated MDMs were exposed to nocodazole (2 µg/ml for 30 min; Sigma-Aldrich), a microtubule-depolymerizing agent, and the phagocytic ability against *A. niger* conidia was examined 1.5 h after challenge by confocal microscopy. The effect of nocodazole on the microtubular network was analyzed after immunostaining, using the anti-human tubulin mouse monoclonal antibody (Molecular Probes) revealed with the secondary Alexa Fluor 488-conjugated anti-mouse immunoglobulin (IgG; Molecular Probes). Cell nuclei were stained with propidium iodide (Sigma-Aldrich). For actin/tubulin double staining, after immunostaining using the anti-human tubulin mouse monoclonal antibody, cells were counterstained for actin using the TRITC-conjugated phalloidin (Sigma-Aldrich).

For the quantitative TEM evaluation of the effect of microtubule destabilization and PKC inhibition on macrophage phagocytic ability, untreated controls and LPS- or Tα1-pretreated MDMs were grown in the presence of nocodazole (Sigma-Aldrich; 2 µg/ml for 30 min) or of the PKC inhibitor staurosporine (Sigma-Aldrich; 0.5 µM for 30 min), respectively, before conidium addition. Two and a half hours after challenge, cells were processed for TEM analysis as described above. A minimum of 50 cells per sample were analyzed.

Phagocytosis Assay Using Complement- or IgG-Opsonized Zymosan Particles

The ingestion by MDMs of fluorescent zymosan particles covalently labeled with two different fluorophores, i.e. Alexa Fluor 488 (Abs/Em: 495/519, green fluorescence) and Alexa Fluor 594 (Abs/Em: 590/617, red fluorescence), and opsonized with IgG (IgG-opsonized zymosan – IgOZ) or with complement (complement-opsonized zymosan – COZ), respectively, was examined by CLSM. Zymosan A BioParticles were reconstituted and used as indicated by the manufacturer. For obtaining IgOZ particles, zymosan particles were opsonized using the opsonizing reagent (Molecular Probes) containing rabbit polyclonal IgG antibodies specific for *Saccharomyces cerevisiae* according to the manufacturer's instruction. For COZ particles, zymosan particles were opsonized with complement components by incubation for 1 h at 37°C in fresh FBS, as described previously [33]. The uniformity of opsonization on the surface of zymosan particles was demonstrated by immunofluorescence microscopy after staining with a TRITC-conjugated anti-rabbit secondary antibody for IgOZ and the anti-C3/C3b mouse monoclonal antibody Ab11871 (Abcam, Cambridge, Mass., USA) with Alexa Fluor 488 anti-mouse IgG for COZ. Two and a half hours after challenge, the number of phagocytized COZ and IgOZ per cell were counted by confocal microscopy. A minimum of 200 cells per sample was examined.

Statistical Analysis

All the quantitative evaluations performed by TEM, SEM and CLSM were performed in a blinded fashion on a minimum number of cells (ranging from 50 to 200) depending on the method used and specified for each assessment in the respective paragraph in the Materials and Methods.

For statistical analysis, a two-tailed Student's *t* test was used. For each evaluation, at least three independent experiments were carried out, and data are given as means ± SD. For all analyses, *p* < 0.05 was used as the critical level of statistical significance.

Results

Effect of Tα1 Activation and Phagocytic Ability of Human MDMs

After a 1-hour exposure to Tα1, cells assumed the typical activated morphology, which was characterized by an enlarged size compared to untreated controls and by the presence of numerous microvillous structures and a rougher surface with prominent filopodia, blebs and ruffling. These characteristics were also exhibited by LPS-stimulated MDMs, which were used as a positive control of macrophage activation (fig. 1). Under these experimental conditions, Tα1-stimulated MDMs showed higher phagocytic activity than LPS-stimulated or control cells against both fluorescent beads and zymosan particles by confocal microscopy (fig. 2). Specifically, following 50 and 100 ng/ml Tα1, the mean numbers of phagocytized beads per cell were 2.4- and 3.5-fold higher than that of LPS-stimulated cells and 16.5- and 23.7-fold that of untreated controls, respectively (fig. 2b), thus demonstrating a dose-dependent effect of the thymic peptide. Accordingly, in MDMs exposed to 100 ng/ml Tα1, the mean numbers of ingested fluorescent zymosan particles were 7.8 and 1.5 times higher than those of untreated controls or LPS-stimulated cells, respectively (fig. 2c, d). In both phagocytosis assays, the percentage of phagocytic cells was also increased by Tα1, but to a lower extent with respect to the number of particles phagocytized per cells (fig. 2b, d)

Effect of Tα1 on the Interaction of Human MDMs with A. niger Conidia

To verify whether Tα1 was able to stimulate the phagocytic ability of MDMs against conidia from pathogenic fungi as well, both Tα1-stimulated (50–100 ng/ml for 1 h) and nonstimulated MDM cultures were challenged with *A. niger* conidia (10 conidia/cell). Phase-contrast microscopy and CLSM performed 30 min and 1.5 h after challenge showed a time-dependent increase in the number of conidia adhering to the cell surface in Tα1-stimulated cultures compared to untreated controls (fig. 3a, b). This observation was also confirmed by SEM (fig. 3c, d), showing that 30 min after challenge the number of adhering conidia was more than 4-fold higher in Tα1-stimulated MDMs (3.5 conidia/cell; fig. 3d) than in untreated control cells (0.8 conidia/cell; fig. 3c). Moreover, 1.5 h after challenge (online suppl. fig. S3), a conspicuous number of conidia completely surrounded by cellular protrusions indicative of phagocytosis were observed in Tα1-stimulated MDMs, unlike what was observed in the untreated controls (arrowheads in online suppl. fig. S3b).

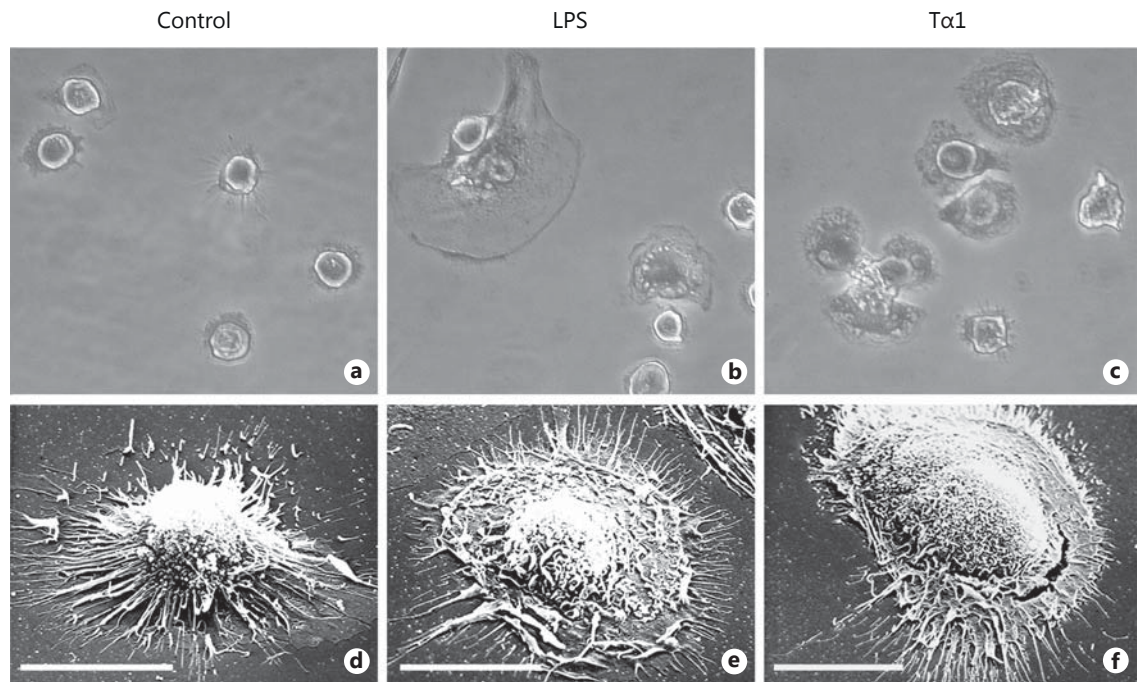


Fig. 1. Morphological features of human MDMs after 1-hour exposure to Tα1. **a–c** Phase-contrast microscopy after Wright-Giemsa staining. Original magnification: $\times 40$. **a** Control MDMs. **b** MDMs stimulated with 0.2 $\mu\text{g}/\text{ml}$ of bacterial LPS. **c** MDMs stimulated with 100 ng/ml Tα1. **d–f** SEM of control (**d**), LPS-stimulated (**e**) and Tα1-stimulated MDMs (**f**). Bars = 20 μm .

Effect of Tα1 on Engulfment and Killing of A. niger Conidia by Human MDMs

TEM analysis evidenced dramatic differences in *A. niger* conidial internalization by Tα1-stimulated and control MDMs (fig. 4). Specifically, 2.5 h after challenge, 85% of Tα1-stimulated MDMs contained *A. niger* conidia (mean: 3.7/cell) compared with 4% of control MDMs (mean: 0.1/cell). Moreover, at this time point, signs of intracellular germination of conidia were observed in control MDMs (fig. 4c), but not in Tα1-stimulated cells (fig. 4d), suggesting that Tα1 may also affect the killing ability of MDMs against conidia. Consistently, 6 h after challenge, the majority of ingested conidia appeared partially digested inside the lysosomes of Tα1-stimulated MDMs (fig. 5b, arrows in fig. 5c), which was different from what was observed in untreated MDMs (fig. 5a). TEM also indicated that Tα1-stimulated phagocytosis occurred by a variation in the classic zipper model [33], in that conidia appeared to sink into the cell with elaboration of small, if any, pseudopodia (fig. 5c, d), and the phagosome membrane was less tightly opposed to the internalized particle, with point-like contact areas separating regions of nontied membrane (arrowheads in fig. 5d).

In accordance with TEM observations, confocal microscopy performed 6 h after challenge showed that Tα1 stimulates the ability of MDMs to process and disassemble the fungal pathogen, since the percentage of conidia colocalizing with both lysosomal (LysoTracker-positive) and proteolytically active (DQ-BSA-positive) intracellular compartments was found significantly higher than in the untreated control cultures (fig. 6a–c).

Twenty-four hours after challenge and after replacement of the culture medium, in Tα1-treated cultures both the number of internalized pathogens per cell and the rate of colocalization with DQ-BSA-positive compartments were reduced by more than 50% compared to the untreated controls (fig. 6d, e).

Effect of Tα1 on Proinflammatory Cytokines and TLR Expression in Human MDMs

In spite of the stimulatory effects of Tα1 on the morphology and phagocytic and fungicidal ability of human MDMs, the transcription levels and release of the proinflammatory cytokines IL-6 and TNF- α were found to be very similar to those of untreated controls but dramatically lower than those of LPS-activated MDMs (fig. 7), at

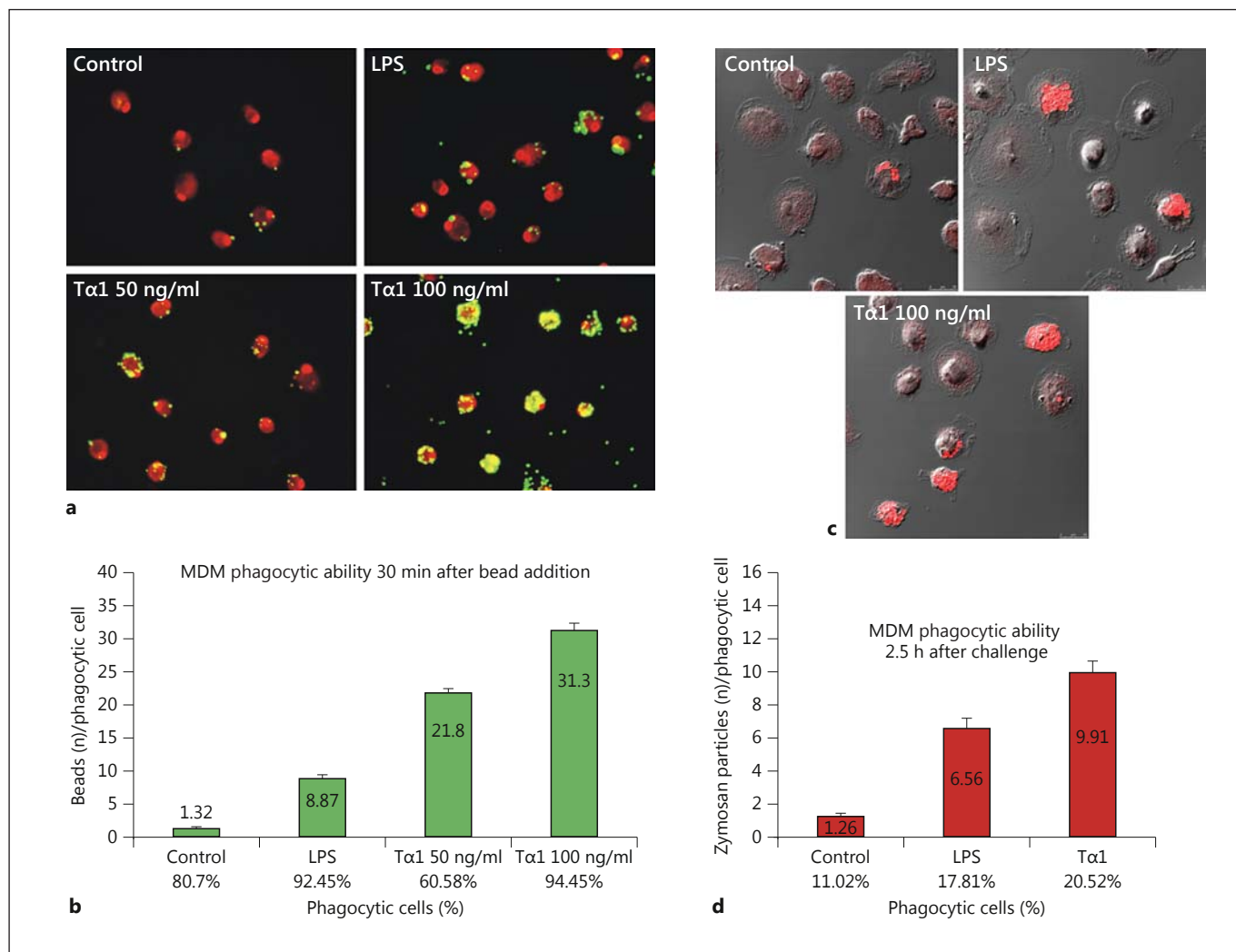


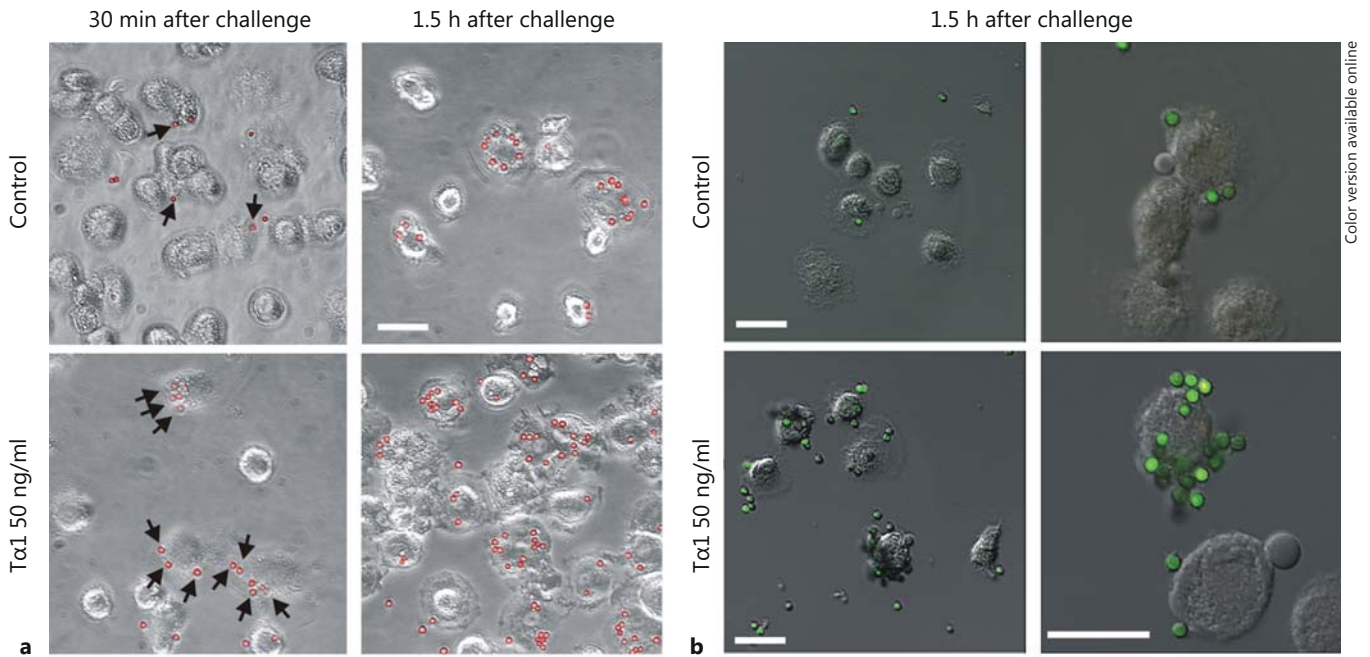
Fig. 2. Effect of Tα1 on the phagocytic activity of human MDMs. **a, b** Phagocytic activity against fluorescent polystyrene beads. **a** Representative CLSM images showing bead uptake (yellow-green hue) in controls, LPS- and Tα1-treated MDMs; cell nuclei were stained with 1 μg/ml propidium iodide (red hue). Original magnification: ×40. **b** Bar graph representing the number of beads per phagocytic cell and the percentage of phagocytic cells. Results are expressed as the mean of three different experiments. Significance vs. control: LPS, $p = 0.00373$; Tα1 50 ng/ml, $p = 0.00158$; Tα1 100 ng/ml, $p = 0.000718$; significance vs. LPS: Tα1 50 ng/ml, $p = 0.0139$;

Tα1 100 ng/ml, $p = 0.00153$. **c, d** Phagocytic activity against nonopsonized zymosan particles covalently labeled with Alexa Fluor 594 (red hue). **c** Representative CLSM images showing zymosan internalization (red hue) in control, LPS-treated and Tα1-treated MDMs. **d** Bar graph representing the number of internalized zymosan particles per phagocytic cell and the percentage of phagocytic cells. Significance vs. control: LPS, $p = 0.001002$; Tα1 100 ng/ml, $p = 0.000722$; significance vs. LPS: Tα1 100 ng/ml, $p = 0.00543$. In both phagocytosis assays, results were obtained by analyzing a minimum of 200 cells per sample. (Colors are available in the online version only.)

least at the early time examined (30 min and 1 h after challenge).

No significant effect on the release of the other proinflammatory and immune-modulating cytokines tested (IL-1β, IL-4, IL-10 and IL-12p70) was recorded for both Tα1 and LPS treatments (data not shown).

In our experimental conditions, the expression levels of TLRs, which are well known mediators of proinflammatory cytokine signaling, appeared not to be influenced by MDM exposure to Tα1 (online suppl. fig. S4). By contrast, TLR 2, TLR 5 and TLR 7 were found to be significantly ($p < 0.05$) upregulated by LPS treatment.



Color version available online

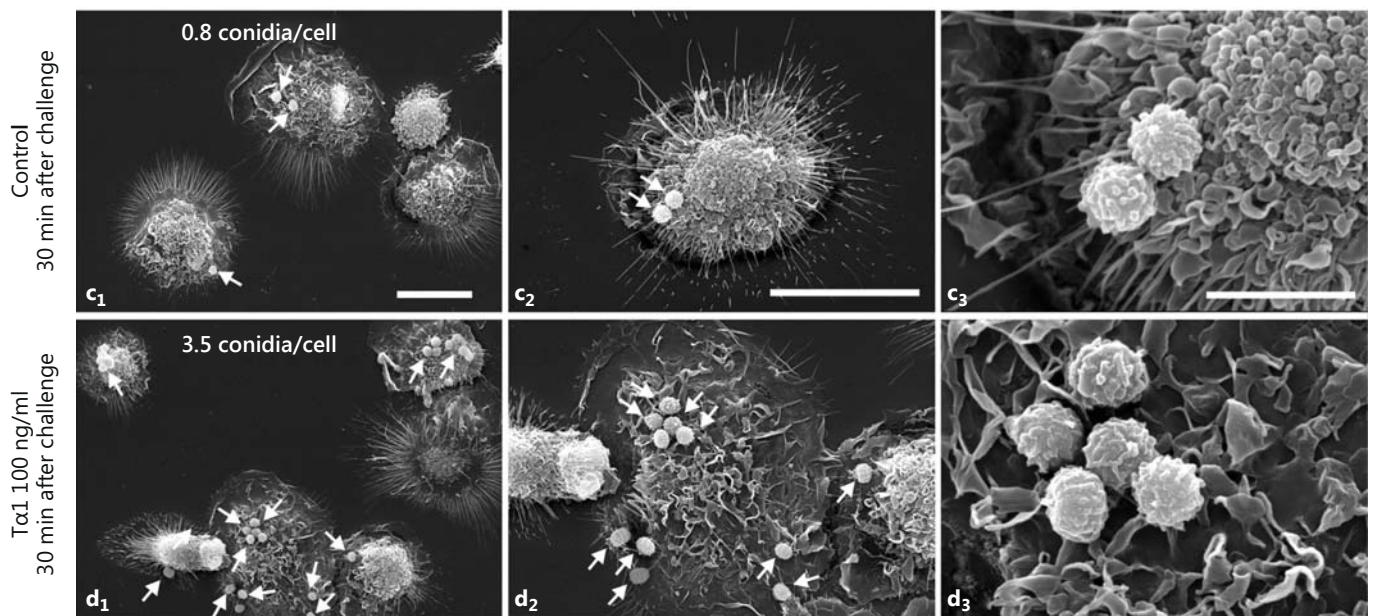


Fig. 3. Effect of Ta1 on the interaction of *A. niger* conidia with human MDMs. **a** Phase-contrast microscopy of control and Ta1-treated MDMs, 30 min and 1.5 h after challenge, showing the interaction with conidia, which were pseudocolored red using the Corel Photo Paint software to enhance contrast. Bar = 20 μm . **b** Confocal microscopy images of *A. niger* conidia, which were stained with Alexa Fluor 488 succinimidyl ester (green hue); merged images with differential interference contrast to visualize cell morphology are shown. Bars = 20 μm . **c, d** SEM of untreated

(**c**) and Ta1-treated MDMs (**d**) 30 min after challenge showing interaction with *A. niger* conidia (arrows). The mean number of adhering conidia on the cell surface for each sample is also reported; quantitative assessment was performed by analyzing, in a blinded fashion, a minimum of 100 cells per sample, and results were expressed as the mean values of three different experiments. Bars = 20 (**c**₁, **d**₁, **c**₂, **d**₂) and 5 μm (**c**₃, **d**₃). (Colors are available in the online version only.)

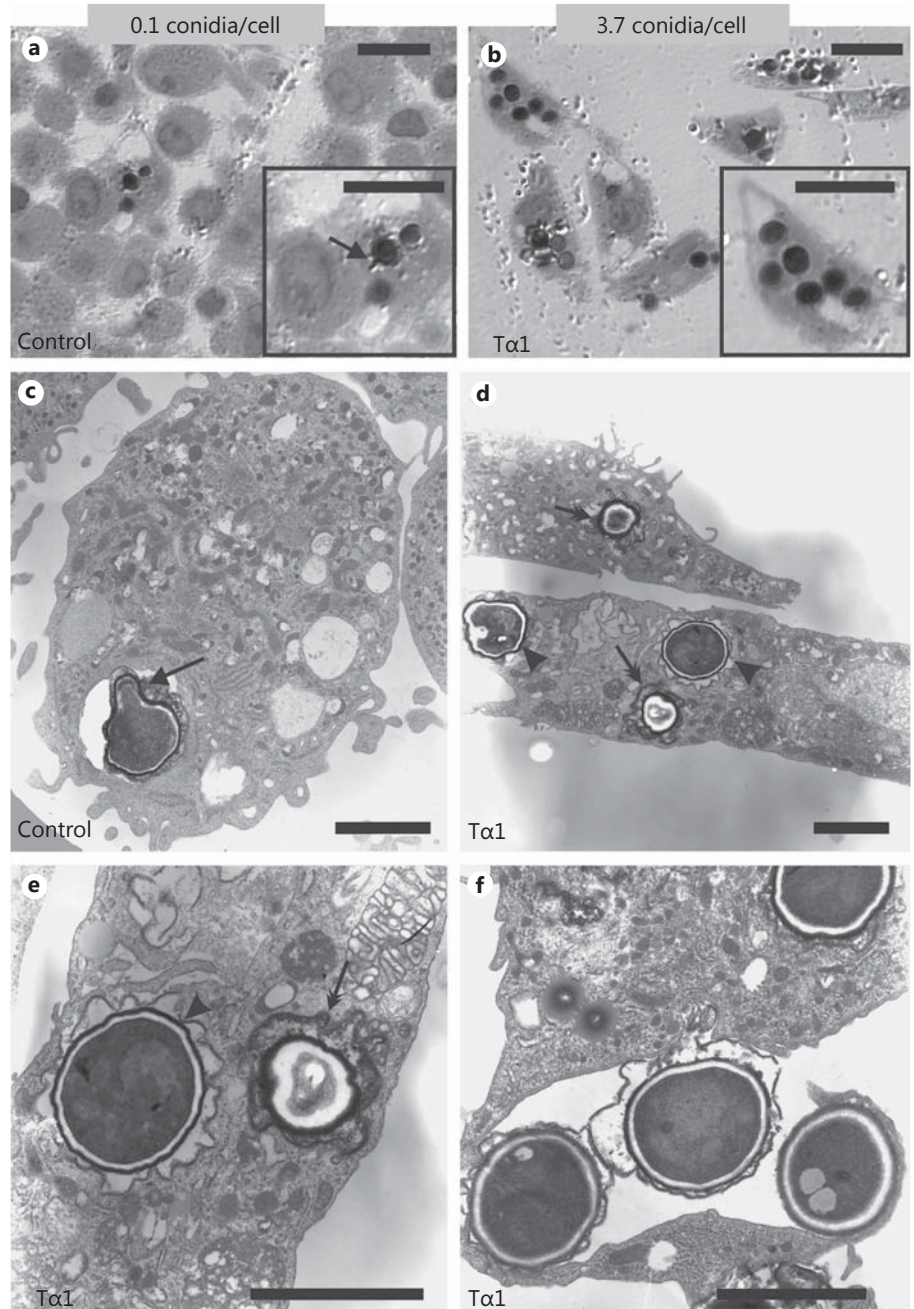


Fig. 4. Effect of Ta1 on the internalization of *A. niger* conidia by human MDMs. TEM images of untreated (**a, c**) and Ta1-treated (100 ng/ml) MDMs (**b, d-f**) 2.5 h after challenge. Both resting (double arrows) and swollen (arrowheads) conidia are internalized (**d, e**). **f** Detail of the engulfment of 3 conidia by an MDM filopodium. **a, c** Arrows point to a germ tube emerging from a conidium. The mean number of ingested conidia/cell for each sample is also reported; the quantitative assessment was done by analyzing, on sequential sections from resin-embedded treated and untreated cells, a minimum of 50 cells per sample by TEM. Bars = 10 (**a, b**) and 3 μ m (**c-f**).

Study of Cytoskeletal Elements Mediating A. niger Conidia Internalization by Ta1-Stimulated MDMs

To determine whether the observed differences in the LPS- or Ta1-stimulated internalization of conidia were associated with the involvement of different cytoskeletal elements mediating phagocytosis, MDMs stimulated or not with Ta1 or LPS were exposed to nocodazole (2 μ g/ml for 30 min), a microtubule-depolymerizing agent, or stau-

rosporine (0.5 μ M for 30 min), an inhibitor of PKC whose activity is required for the formation of actin microfilament at the phagosome level [34]. MDMs were then challenged with *A. niger* (10 conidia/cell) and examined by CLSM and TEM up to 2.5 h after the fungal challenge.

CLSM and TEM (online suppl. fig. S5; fig. 8) showed that damaging of the microtubular network by nocodazole almost completely inhibited internalization of

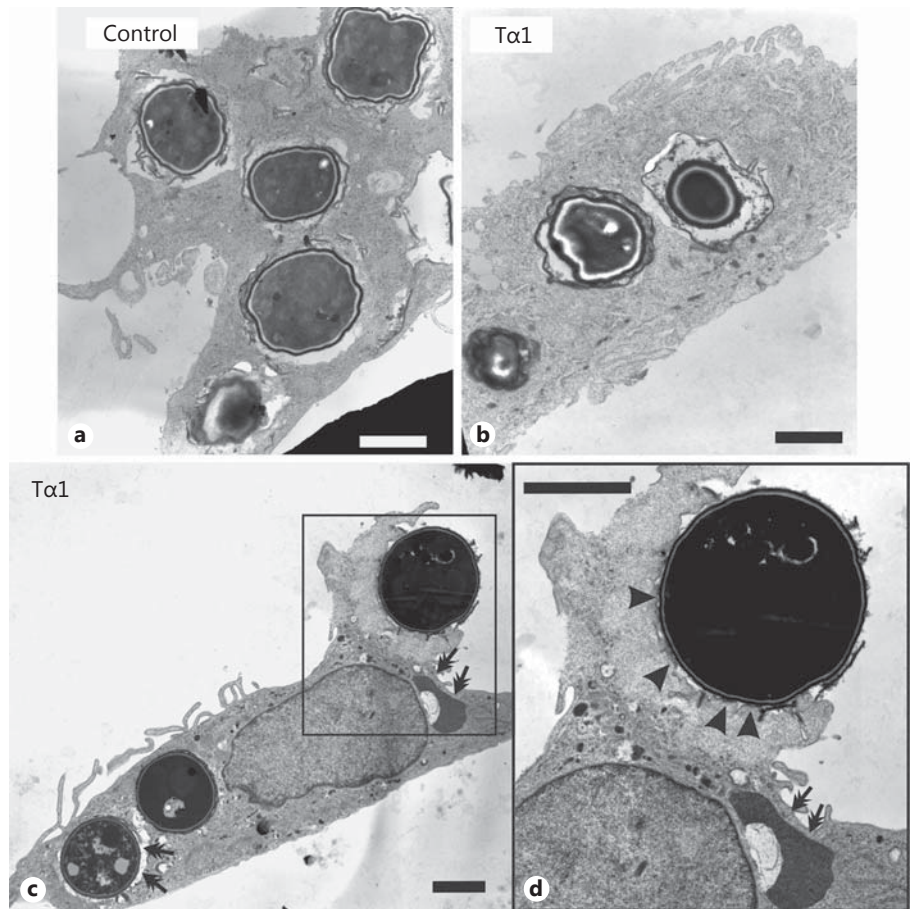


Fig. 5. Effect of Tα1 on the ability of human MDMs to kill *A. niger* conidia. TEM images of untreated (a) and Tα1-treated (100 ng/ml) MDMs (b–d) 6 h after the conidial challenge. Double arrows point to conidia partially digested inside lysosomes. d A swollen conidium sinking into the cells with elaboration of small pseudopodia (arrowheads). Bars = 2 μm.

conidia stimulated by Tα1 (0.12 vs. 3.22 internalized conidia/cell in the absence of nocodazole), but not that induced by LPS treatment (1.6 vs. 1.3 conidia/cell without nocodazole). Tα1-stimulated internalization of *Aspergillus* conidia was also dramatically reduced by staurosporine (to 0.2 internalized conidia/cell), while the phagocytic ability of the LPS-stimulated MDMs was affected to a lower extent (0.5 internalized conidia/cell).

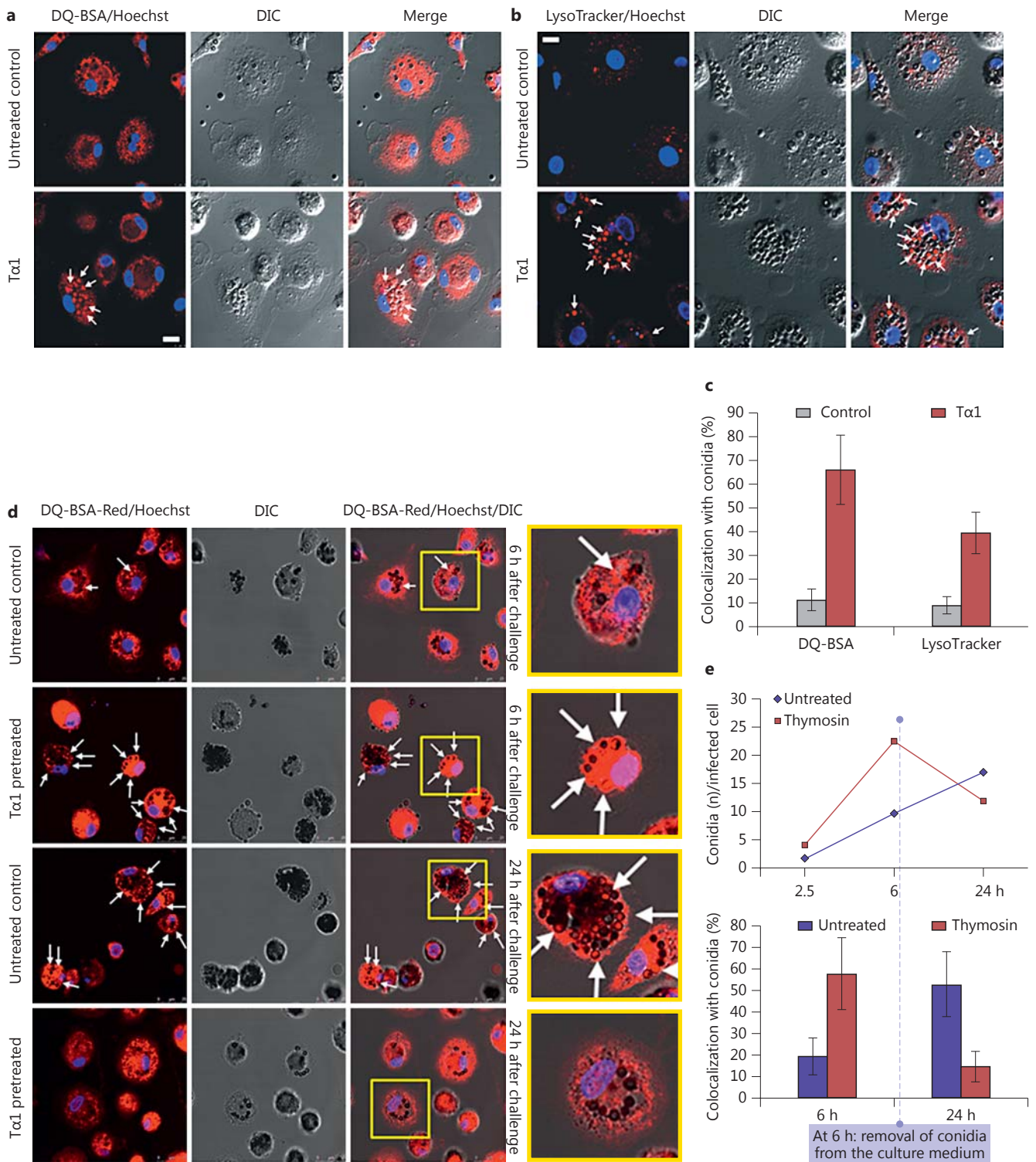
These results were confirmed by a phagocytosis assay which used unopsonized fluorescent zymosan particles (fig. 8e, right graph), thus proving that the observed effect was not specific for *A. niger* conidia.

In addition, whereas the actin microfilament network was similarly affected by LPS or Tα1 stimulation, Tα1 provoked a more dramatic reorganization of microtubular filaments than LPS (fig. 9a), strongly suggesting that tubulin plays an important role in Tα1-stimulated macrophage activation. Moreover, vinculin and F-actin appeared to be differently associated with phagosomes in Tα1- or LPS-stimulated MDMs. Consistently, in Tα1-

stimulated MDMs, the recruitment of these cytoskeletal components to the periphagosomal cytoplasm predominantly exhibited a punctate distribution (fig. 9b), with vinculin and actin assembling and colocalizing into focal structures around the membrane of Tα1-induced phagosome (arrows in fig. 9c). Conversely, in LPS-stimulated cultures, periphagosomal vinculin and F-actin displayed both a diffuse pattern and a punctate distribution (data not shown).

Assessment of the Involvement of Complement Receptor in Tα1-Stimulated Phagocytosis

Finally, a phagocytosis assay which used fluorescent COZ or IgOZ, respectively, was performed in order to discriminate whether Tα1 stimulates complement receptor (CR)- or the IgG receptor (FcR)-mediated phagocytosis. For this assay, Alexa Fluor 488-IgOZ (green hue) and Alexa Fluor 594-COZ (red hue) were simultaneously added (20 conidia/cell, COZ/IgOZ ratio: 1:1) to the MDM cultures which had been previously exposed to Tα1 (1 h



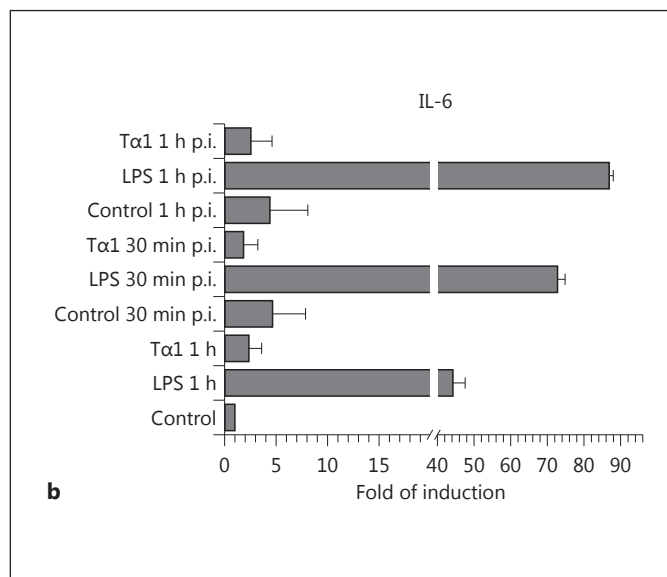
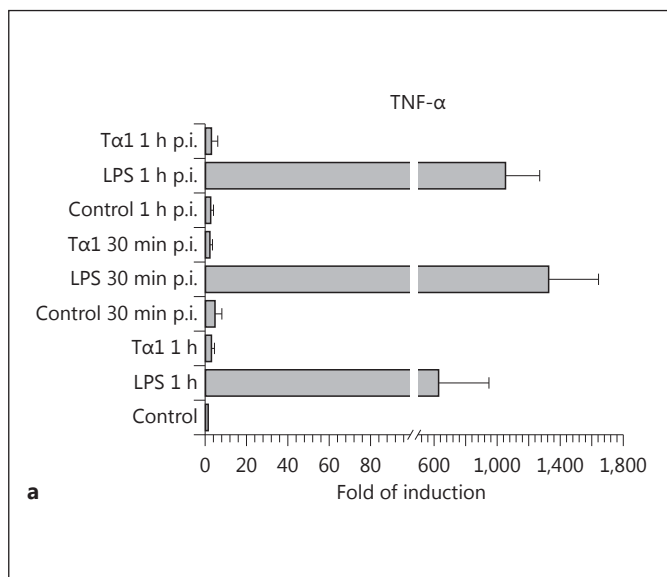


Fig. 7. Effect of Ta1 on the transcription levels and release of TNF- α and IL-6 by human MDMs before and after challenge with *A. niger* conidia. **a, b** Cytokine expression by RT-PCR; results represent the mean fold of induction found in 4 independent experiments using MDMs from different donors. p.i. = after infection. **c** Analysis by cytometric bead array of TNF- α and IL-6 release. In both analyses, significance for all the treated samples against the respective controls: $p < 0.001$.

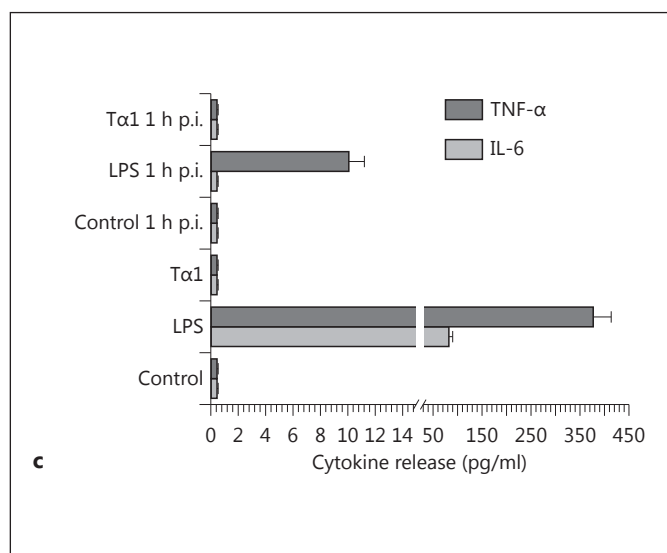


Fig. 6. Effect of Ta1 on the ability of human MDMs to process and disassemble *A. niger* conidia. **a, b** Confocal microscopic images of Ta1-pretreated MDMs and untreated controls 6 h after conidial challenge; cells were loaded with LysoTracker-Red or DQ-BSA-Red probes for staining of lysosomal (**b**) and proteolytically active (**a**) compartments, respectively. Merged images of DIC and LysoTracker or DQ-BSA fluorescence (red) are shown. Cell nuclei were counterstained with Hoechst (blue hue). Bar = 10 μ m. **c** Solid bar graph reporting the percentage of internalized conidia colocalizing with LysoTracker or DQ-BSA-positive compartments (arrows), in Ta1-pretreated samples and untreated controls. A

minimum of 200 cells per sample were observed. Significance for Ta1 vs. control: LysoTracker, $p = 0.0049$; DQ-BSA, $p = 0.0202$. **d** Confocal microscopic representative images of DQ-BSA-loaded MDMs, 6 h after conidia challenge and after an additional 18 h of culture in conidia-free medium (24 h after challenge). **e** Quantitative assessment of fungicidal ability in control and Ta1-treated MDMs performed by evaluating the number of internalized pathogens per infected cells (top panel) as well as the percentage of internalized conidia colocalizing with DQ-BSA-positive compartments (bottom panel). (Colors are available in the online version only.)

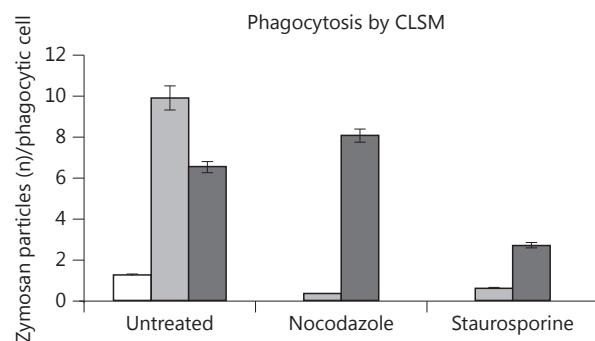
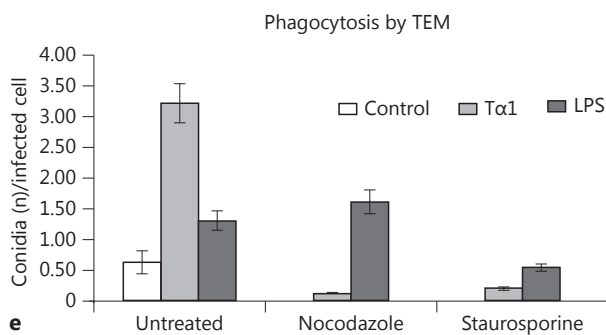
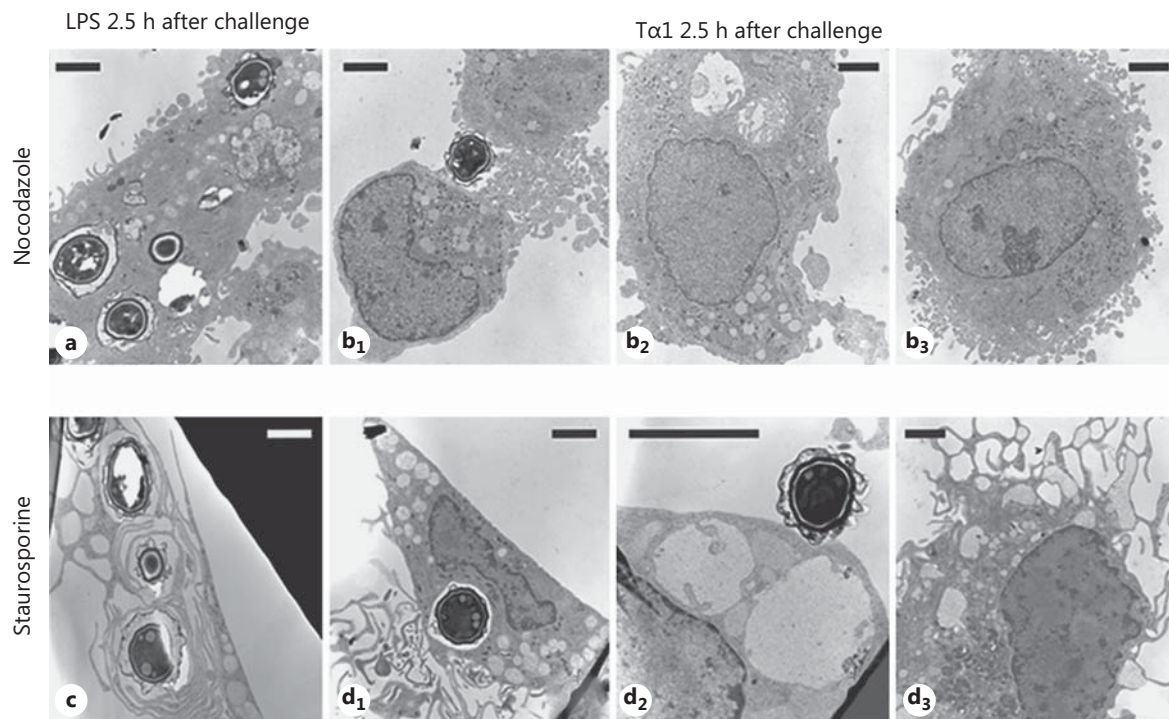


Fig. 8. Effect of microtubule destabilization by nocodazole and of PKC inhibition by staurosporine on the phagocytic activity of Tα1-stimulated human MDMs. **a–d** TEM images showing the *A. niger* conidial uptake in LPS-stimulated (**a, c**) and Tα1-stimulated MDMs (**b, d**) in the presence of nocodazole (**a, b**) or staurosporine (**c, d**); **b₁, b₂, b₃, d₁, d₂, d₃** Different representative cells in Tα1-stimulated MDMs. Bars = 2 μm. **e** Phagocytosis of *A. niger* conid-

ia by Tα1- or LPS-stimulated MDMs in the absence and presence of nocodazole or staurosporine; the solid bar graphs report the number of internalized conidia evaluated by TEM (left graph) and the number of nonopsonized zymosan particles evaluated by CLSM (right graph). Significance vs. untreated control: Tα1 + nocodazole, $p = 0.0156927$; LPS + nocodazole, $p = 0.121706$; Tα1 + staurosporine, $p = 0.017701$; LPS + staurosporine, $p = 0.037381$.

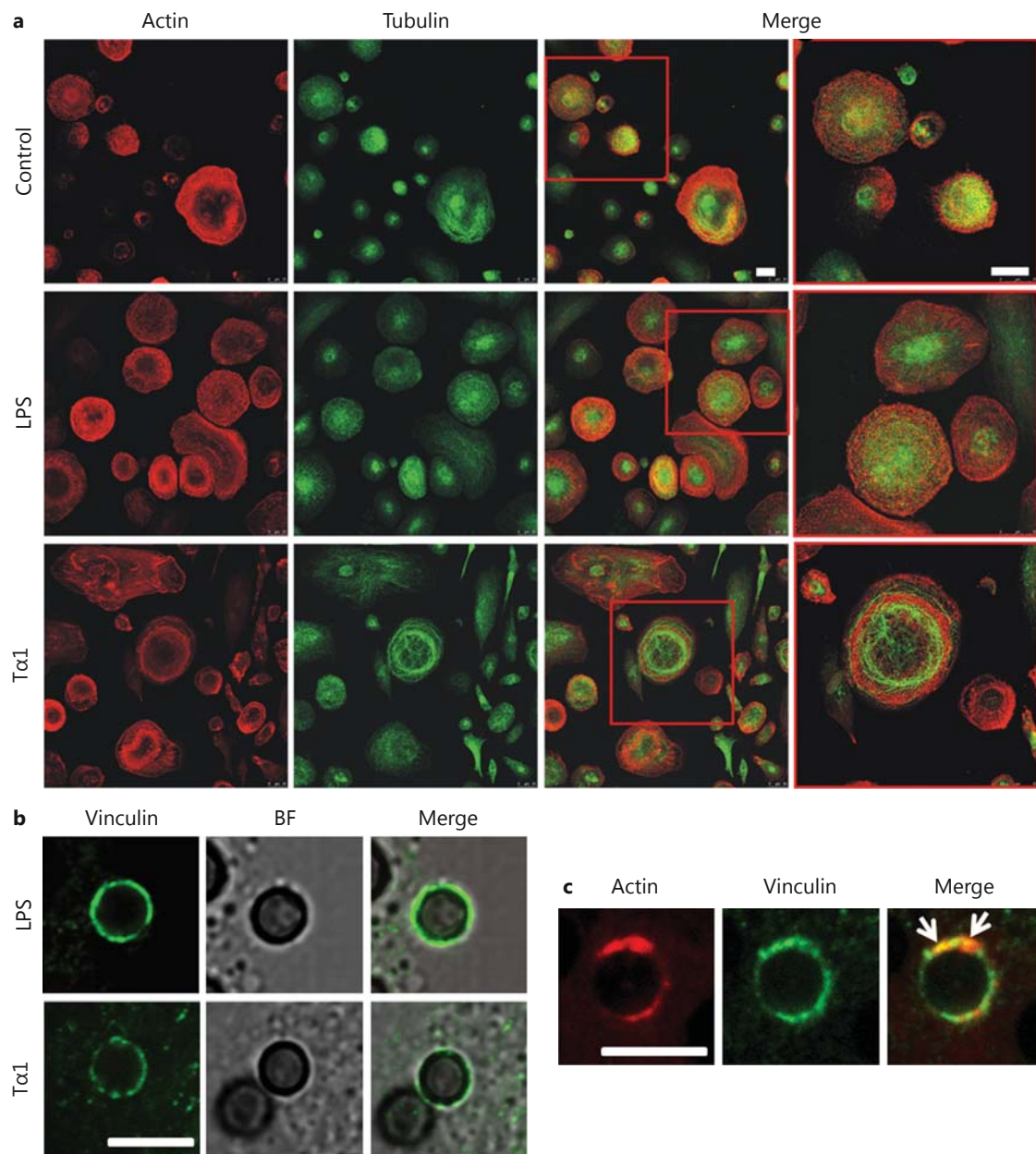


Fig. 9. Effect of Ta1 on cytoskeletal components of human MDMs by CLSM. **a** Images showing the organization of actin and tubulin in Ta1- or LPS-stimulated MDMs. Cells were double stained for F-actin using TRITC-phalloidin (red hue) and for tubulin using the specific monoclonal antibody (green hue). Bars = 25 μ m. **b, c** Recruitment of vinculin and F-actin to the periphagosomal cytoplasm. **b** Association of vinculin with conidium-internalizing phagosomes in Ta1- or LPS-stimulated MDMs 1 h after challenge.

Both cells and conidial morphology were visualized in a bright field modality (BF). **c** Vinculin and actin assembly on phagosome membrane in Ta1-stimulated MDMs. Cells were double stained for F-actin using TRITC-phalloidin (red hue) and for vinculin using the specific monoclonal antibody (green hue); arrows point to vinculin and actin colocalization into focal structures around the membrane of Ta1-induced phagosome. Bars = 5 μ m. (Colors are available in the online version only.)

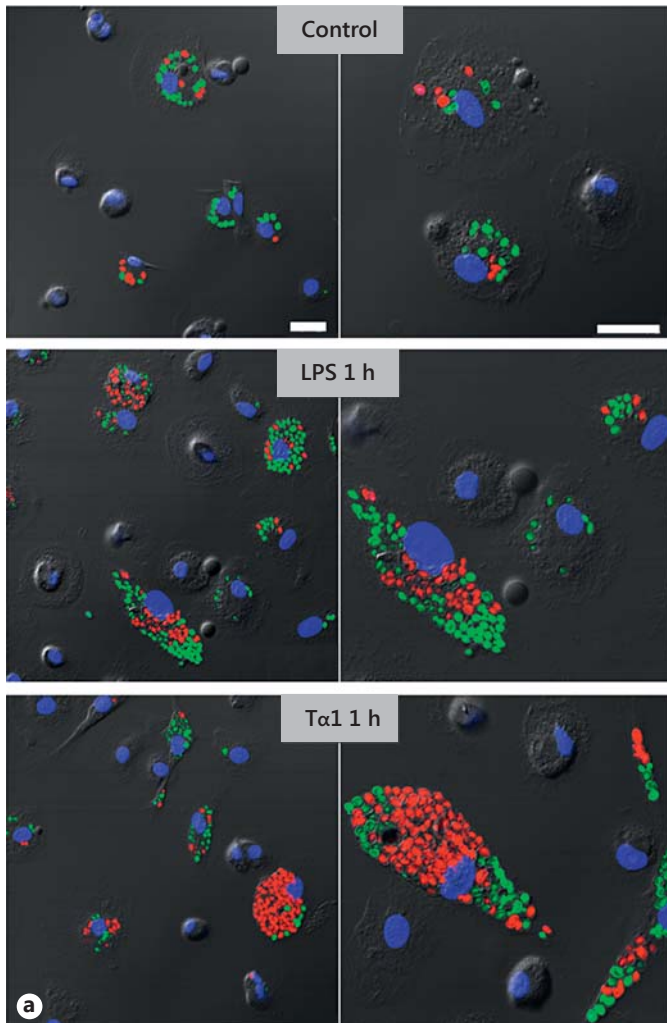
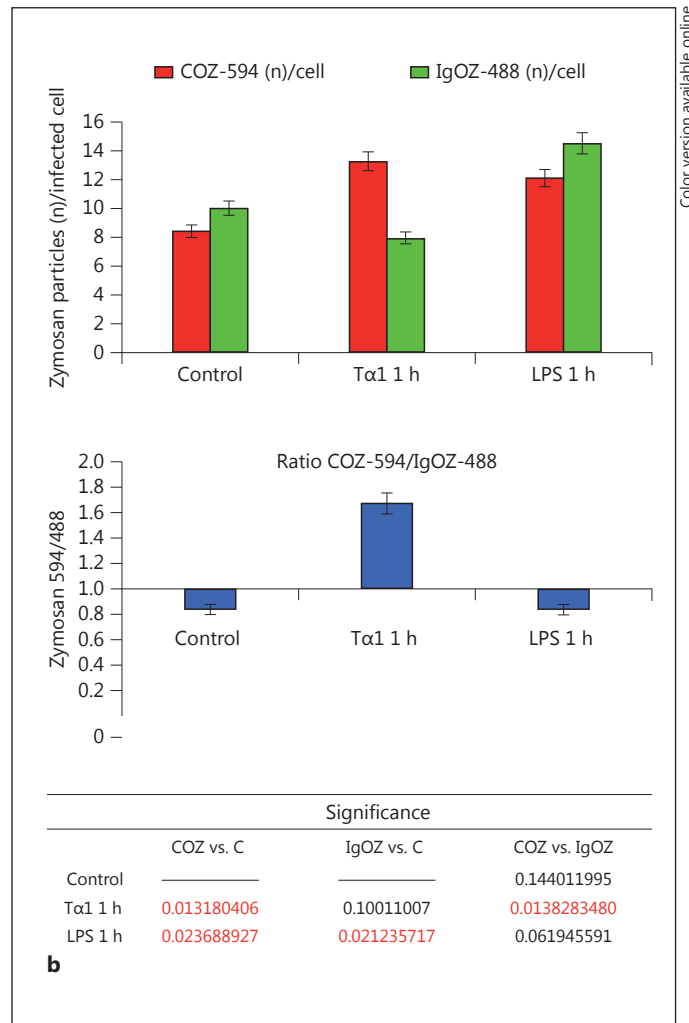


Fig. 10. CR involvement in Tα1-stimulated phagocytosis. **a** A representative field of MDM cultures during phagocytosis of fluorescent COZ or IgOZ by CLSM. Alexa Fluor 594-COZ (red hue) and Alexa Fluor 488-IgOZ (green hue) were simultaneously added (20 total conidia/cell, ratio COZ/IgOZ 1:1) to MDMs pretreated or not 1 h with Tα1 or LPS; for each sample, images recorded at two different magnifications are reported. Bars = 25 μm. **b** Quantitative



Color version available online

at 100 ng/ml) or LPS (1 h at 0.2 μg/ml). As reported in fig. 10a, LPS treatment promoted the internalization of both COZ and IgOZ particles with a ratio of

$$\frac{COZ(n)}{IgOZ(n)} < 1,$$

which was comparable to that of the untreated controls (number of IgOZ about 1.2-fold higher than that of COZ).

analysis of the above phagocytosis assay; results are expressed as numbers of zymosan particles per phagocytic cell (top bar graph) and as ratio number of COZ/number of IgOZ: values >1 indicate that COZ particles are internalized at higher numbers than the IgOZ particles. Statistical significance by two-tailed Student's t test is reported at the bottom table. C = Control. (Colors are available in the online version only.)

Conversely, in Tα1-treated cultures, COZ particles were internalized in a number which was about 2-fold higher than IgOZ particles with a ratio of

$$\frac{COZ(n)}{IgOZ(n)} > 1,$$

demonstrating that Tα1 mainly acts by promoting the CR-mediated phagocytosis.

Discussion

The modulatory activity of T α 1 on cells of the innate immune system, including PMNs, PBMCs and DCs, has been extensively described, but the mechanism(s) of action of the peptide remain not yet completely understood.

Here we show that, upon T α 1 stimulation, human MDMs undergo an early and powerful morphological activation whose features strictly resemble those of LPS-stimulated MDMs, which were used as a positive control. However, the phagocytic ability of T α 1-stimulated MDMs against fungal and nonfungal agents is higher than that of LPS-stimulated cells. The effects of T α 1 on MDM morphology and phagocytic ability occur at a time when both the transcription levels and the release of TNF- α and IL-6 are near to those of the untreated controls and dramatically lower than those of the LPS-stimulated MDMs. It seems, therefore, that in our experimental culture conditions the T α 1-stimulated phagocytosis is mediated by a mechanism that is not coupled to an inflammatory response, at least at the early times examined. Accordingly, at these times, the transcription levels of all the TLRs studied appear to be unmodified or slowly downregulated by T α 1 treatment, whereas TLR 2, TLR 5 and TLR 7 are significantly upregulated by LPS stimulation.

We show that T α 1 is not only substantially involved in the interaction of human MDMs with conidia but also increases the ability of MDMs to internalize, process and disassemble the fungal pathogen, so that 6 h after challenge the majority of the internalized conidia appear proteolytically processed within the lysosomes of T α 1-stimulated cells, but not in those of untreated controls. Taken together, these results clearly indicate that T α 1-induced stimulation is a highly efficient process triggered in a short time considering that the addition of the peptide to the cultures preceded the fungal challenge by only 1 h.

We also report that T α 1- and LPS-induced stimulation of MDM phagocytosis occurs by means of different mechanisms of action. First, the T α 1-stimulated internalization of *A. niger* conidia or of nonopsonized zymosan particles, but not those stimulated by LPS, requires the integrity of the microtubule network, as demonstrated by inhibition experiments with the microtubule-depolymerizing agent nocodazole. Second, tubulin seems to play a more predominant role in T α 1-induced MDM activation than in the LPS-induced one. Consistently, preliminary results obtained in our laboratory have documented that tubulin is highly polarized in T α 1-treated MDMs (data not shown), confirming previous reports about the effect

of other thymic preparations on human monocyte polarization [35, 36]. Moreover, given the well-known function of microtubules in facilitating the fusion between phagosomes and endocytic organelles to form the phagolysosome [37], the dramatic reorganization of the microtubular network in T α 1-stimulated cultures could be one of the factors responsible for the augmented MDM ability to process and disassemble the *A. niger* conidia. Third, the recruitment of F-actin and vinculin to the periphagosomal cytoplasm exhibits a punctate pattern for T α 1, and both a diffuse pattern and a punctate distribution for LPS. Moreover, in our experimental conditions, T α 1-stimulated phagocytosis is highly dependent on PKC-mediated phosphorylation, while that promoted by LPS is influenced to a lower extent, as reflected by the addition of the PKC inhibitor staurosporine to the cultures. Finally, the internalization of *A. niger* conidia induced by T α 1 mainly occurs by a variation in the classic zipper model previously described [33, 38], with the phagosome membrane loosely opposed to the internalized particle and point-like contact areas separating regions of nontied membrane.

It is known that macrophages detect infectious organisms via a plethora of receptors, phagocytize them and orchestrate appropriate host responses. Specifically, differentiated macrophages, such as resident lung phagocytes, express high densities of immunoglobulin receptor (FcR), CR, mannose receptor (MR) and several types of scavenger receptors to facilitate phagocytosis of opsonized and nonopsonized particles [2, 39]. Infectious agents are mainly phagocytized by CRs after a relatively nonspecific opsonization with complement proteins or by FcR after a specific opsonization with antibodies. FcR-mediated phagocytosis is tightly coupled to the production and secretion of proinflammatory cytokines and reactive oxygen intermediates [40], which may be in contrast to CR-mediated phagocytosis. Furthermore, only in the CR-mediated internalization, particles appear to sink into the cell with elaboration of small, if any, pseudopodia [38]; intact microtubules are required and point-like structures rich in vinculin, F-actin, α -actinin, paxillin and phosphotyrosine-containing proteins are enriched in discrete regions or foci on the phagosome membrane [39]. The formation of these punctate structures is dependent on active PKC, and PKC inhibitors block phagocytosis of complement-opsonized particles [33, 41]. MR, which recognizes mannose and fucose on the pathogen surface, possesses broad pathogenic specificity, but, differently from the CR- and FcR-mediated phagocytosis, vinculin is not recruited to the MR phagosome. Moreover, MR-me-

diated phagocytosis is a proinflammatory process which is tightly coupled to the generation of inflammatory mediators [33].

In this scenario, our data strongly suggest that Tα1 implements pathogen internalization, which mainly stimulates CR-mediated phagocytosis, as definitively confirmed by means of phagocytosis experiments performed with both COZ and IgOZ particles.

It is known that phagocytosis is an extraordinarily complex process and that many molecules which have a role in particle ingestion also participate in signaling events that lead to gene transcription and protein secretion, alterations in cell morphology and activation of antimicrobial mechanisms. The extensive overlap in signaling molecules used for these different processes and the concomitant recruitment of these molecules at the phagosome level make it likely that the different signaling pathways interact functionally [2]. Thus, activation of different phagocytic receptors might not only be dependent *sensu strictiori* on the type of ligand or activator molecule, but also on the 'activation state' of the host cell, which in turn is dependent both on its level of differentiation and on the experimental conditions of testing. This might also explain the differences in the expression of the proinflammatory cytokine genes found by us in mature macrophages from peripheral blood, and those reported by others in bone marrow-derived macrophages following Tα1 treatment [29].

Finally, it has been reported that whereas FcRs are constitutively active for phagocytosis, the ability of CRs to

promote phagocytosis is a regulated process [42]. Consistently, CRs appear to exist in two states: an 'active' state, i.e. capable of both binding and internalizing foreign particles, or an 'inactive' one, i.e. capable of only binding but not internalizing particles in the absence of additional stimuli, such as PMA, TNF-α, GM-CSF, or attachment to laminin- or fibronectin-coated substrata [33]. In this context, the possibility that Tα1 acts as an additional stimulus capable of activating CRs for ingestion cannot be ruled out. Therefore, our findings add to recent evidence of multiple pathways engaged by Tα1 in the stimulation of immune effector cells and reinforce the concept of its pleiotropy [43].

In conclusion, we show that Tα1 implements pathogen internalization and killing by human mature MDMs in a short time and with high efficiency. The above findings might have profound implications for innate immune responses during early stages of pathogen infection. For the first time, we also provide evidence that in mature macrophages this effect is mediated by CR activation. Further molecular studies aimed to elucidate the observed phenomena are in progress in our laboratories.

Acknowledgments

This work was supported by grants from the Italian Ministry of University and Research (MIUR): Research Projects of National Interest 2008 to E.G., and MIUR Prot. 10484 to P.S.-V. and E.G. We thank Martino Tony Miele for assistance in text editing.

References

- 1 Stafford JL, Neumann NF, Belosevic M: Macrophage-mediated innate host defence against protozoan parasites. *Crit Rev Microbiol* 2002; 28:187–248.
- 2 Underhill DM, Ozinsky A: Phagocytosis of microbes: complexity in action. *Annu Rev Immunol* 2002;20:825–852.
- 3 Gougerot-Pocidallo MA, el Benna J, Elbim C, Chollet-Martin S, Dang MC: Regulation of human neutrophil oxidative burst by pro- and anti-inflammatory cytokines. *Soc Biol* 2002; 196:37–46.
- 4 Goldstein AL, Guha A, Zatz MM, Hardy MA, White A: Purification and biological activity of thymosin, a hormone of the thymus gland. *Proc Natl Acad Sci USA* 1972;69:1800–1803.
- 5 Low TL, Goldstein AL: The chemistry and biology of thymosin. II. Amino acid sequence analysis of thymosin alpha1 and polypeptide beta1. *J Biol Chem* 1979;254:987–995.
- 6 Wang SS, Makofske R, Bach A, Merrifield RB: Automated solid phase synthesis of thymosin alpha 1. *Int J Pept Protein Res* 1980;15:1–4.
- 7 Billich A: Thymosin alpha1, SciClone Pharmaceuticals. *Curr Opin Investig Drugs* 2002; 3:698–707.
- 8 Rasi G, Di Virgilio D, Mutchnick MG, Colella F, Sinibaldi-Vallebona P, Pierimarchi P, Valli B, Garaci E: Combination thymosin alpha 1 and lymphoblastoid interferon treatment in chronic hepatitis C. *Gut* 1996;39:679–683.
- 9 Rasi G, Mutchnick MG, Di Virgilio D, Sinibaldi-Vallebona P, Pierimarchi P, Colella F, Favalli C, Garaci E: Combination low-dose lymphoblastoid interferon and thymosin alpha 1 therapy in the treatment of chronic hepatitis B. *J Viral Hepat* 1996;3:191–196.
- 10 Garaci E, Pica F, Serafino A, Balestrieri E, Matteucci C, Moroni G, Sorrentino R, Zonfrillo M, Pierimarchi P, Sinibaldi-Vallebona P: Thymosin α1 and cancer: action on immune effector and tumor target cells. *Ann NY Acad Sci* 2012;1269:26–33.
- 11 Wara DW, Goldstein AL, Doyle NE, Amman AJ: Thymosin activity in patients with cellular immunodeficiency. *N Engl J Med* 1975;292: 70–74.
- 12 Garaci E, Rocchi G, Perroni L, D'Agostini C, Soscia F, Grelli S, Mastino A, Favalli C: Combination treatment with zidovudine, thymosin alpha 1 and interferon-alpha in human immunodeficiency virus infection. *Int J Clin Lab Res* 1994;24:23–28.
- 13 Ershler WB, Gravenstein S, Geloo ZS: Thymosin alpha 1 as an adjunct to influenza vaccination in the elderly: rationale and trial summaries. *Ann NY Acad Sci* 2007;112:375–384.

- 14 Goldstein AL, Badamchian M: Thymosins: chemistry and biological properties in health and disease. *Expert Opin Biol Ther* 2004;4: 559–573.
- 15 Favalli C, Jezzi T, Mastino A, Rinaldi-Garaci C, Riccardi C, Garaci E: Modulation of natural killer activity by thymosin alpha 1 and interferon. *Cancer Immunol Immunother* 1985;20:189–192.
- 16 Garaci E, Mastino A, Pica F, Favalli C: Combination treatment using thymosin alpha 1 and interferon after cyclophosphamide is able to cure Lewis lung carcinoma in mice. *Cancer Immunol Immunother* 1990;32:154–160.
- 17 Garaci E, Pica F, Rasi G, Favalli C: Thymosin alpha1 in the treatment of cancer: from basic research to clinical application. *Int J Immunopharmacol* 2000;22:1067–1076.
- 18 Mastino A, Favalli C, Grelli S, Rasi G, Pica F, Goldstein AL, Garaci E: Combination therapy with thymosin alpha 1 potentiates the antitumor activity of interleukin-2 with cyclophosphamide in the treatment of the Lewis lung carcinoma in mice. *Int J Cancer* 1992;50: 493–499.
- 19 Sztejn MB, Serrate SA, Goldstein AL: Modulation of interleukin 2 receptor expression on normal human lymphocytes by thymic hormones. *Proc Natl Acad Sci USA* 1986;83: 6107–6111.
- 20 Bistoni F, Marconi P, Frati L, Bonmassar E, Garaci E: Increase of mouse resistance to *Candida albicans* infection by thymosin alpha 1. *Infect Immun* 1982;36:609–614.
- 21 Bistoni F, Baccharini M, Blasi E, Riccardi C, Marconi P, Garaci E: Modulation of polymorphonucleate-mediated cytotoxicity against *Candida albicans* by thymosin alpha 1. *Thymus* 1985;7:69–84.
- 22 Ishitsuka H, Umeda Y, Nakamura J, Yagi Y: Protective activity of thymosin against opportunistic infections in animal models. *Cancer Immunol Immunother* 1983;14:145–150.
- 23 Tzehoval E, Sztejn MB, Goldstein AL: Thymosins alpha 1 and beta 4 potentiate the antigen-presenting capacity of macrophages. *Immunopharmacology* 1989;18:107–113.
- 24 Hu SK, Badamchian M, Mitcho YL, Goldstein AL: Thymosin enhances the production of IL-1 alpha by human peripheral blood monocytes. *Lymphokine Res* 1989;8:203–214.
- 25 Shrivastava P, Singh SM, Singh N: Activation of tumor-associated macrophages by thymosin alpha 1. *Int J Immunopathol Pharmacol* 2004;17:39–47.
- 26 Giuliani C, Napolitano G, Mastino A, Di Vincenzo S, D'Agostini C, Grelli S, Bucci I, Singer DS, Kohn LD, Monaco F, Garaci E, Favalli C: Thymosin-alpha1 regulates MHC class I expression in FRTL-5 cells at transcriptional level. *Eur J Immunol* 2000;30:778–786.
- 27 Knutsen AP, Freeman JJ, Mueller KR, Roodman ST, Bouhasin JD: Thymosin-alpha1 stimulates maturation of CD34+ stem cells into CD3+4+ cells in an in vitro thymic epithelia organ coculture model. *Int J Immunopharmacol* 1999;21:15–26.
- 28 Romani L, Bistoni F, Gaziano R, Bozza S, Montagnoli C, Perruccio K, Pitzurra L, Bellocchio S, Velardi A, Rasi G, Di Francesco P, Garaci E: Thymosin alpha 1 activates dendritic cells for antifungal Th1 resistance through toll-like receptor signaling. *Blood* 2004;103: 4232–4239.
- 29 Zhang P, Chan J, Dragoi AM, Gong X, Ivanov S, Li Z-W, Chuang T, Tuthill C, Wan Y, Karin M, Chu W-M: Activation of IKK by thymosin alpha 1 requires the TRAF6 signaling pathway. *EMBO Rep* 2005;6:531–537.
- 30 Serafino A, Moroni N, Psaila R, Zonfrillo M, Andreola F, Wannenes F, Mercuri L, Rasi G, Pierimarchi P: Anti-proliferative effect of atrial natriuretic peptide on colorectal cancer cells: evidence for an Akt-mediated cross-talk between NHE-1 activity and Wnt/ β -catenin signaling. *Biochim Biophys Acta* 2012;1822: 1004–1018.
- 31 Serafino A, Sinibaldi Vallebona P, Andreola F, Zonfrillo M, Mercuri L, Federici M, Rasi G, Garaci E, Pierimarchi P: Stimulatory effect of Eucalyptus essential oil on innate cell-mediated immune response. *BMC Immunol* 2008, DOI: 10.1186/1471-2172-9-17.
- 32 Rodriguez-Caballero A, Garcia-Montero AC, Bueno C, Almeida J, Varro R, Chen R, Pandiella A, Orfao A: A new simple whole blood flow cytometry-based method for simultaneous identification of activated cells and quantitative evaluation of cytokines released during activation. *Lab Invest* 2004;84:1387–1398.
- 33 Allen LH, Aderem A: Molecular definition of distinct cytoskeletal structures involved in complement- and Fc receptor-mediated phagocytosis in macrophages. *J Exp Med* 1996;184:627–637.
- 34 Allen LH, Aderem A: A role for MARCKS, the α isozyme of protein kinase C and myosin I in zymosan phagocytosis by macrophages. *J Exp Med* 1995;182:829–840.
- 35 Tas MP, Simons PJ, Balm FJ, Drexhage HA: Depressed monocyte polarization and clustering of dendritic cells in patients with head and neck cancer: in vitro restoration of this immunosuppression by thymic hormones. *Cancer Immunol Immunother* 1993;36:108–114.
- 36 Kerrebijn JD, Simons PJ, Tas M, Balm AJ, Drexhage HA: In vivo effects of thymostimulin treatment on monocyte polarization, dendritic cell clustering and serum p15E-like trans-membrane factors in operable head and neck squamous cell carcinoma patients. *Eur Arch Otorhinolaryngol* 1995;252:409–416.
- 37 Goldstein IS, Hoffstein J, Gallin J, Weissmann G: Mechanisms of lysosomal enzyme release from human leukocytes: microtubule assembly and membrane fusion induced by a component of complement. *Proc Natl Acad Sci USA* 1973;70:2916–2920.
- 38 Kaplan G: Differences in the mode of phagocytosis with Fc and C3 receptors in macrophages. *Scand J Immunol* 1977;6:797–807.
- 39 Aderem A, Underhill DM: Mechanisms of phagocytosis in macrophages. *Annu Rev Immunol* 1999;17:593–623.
- 40 Wright SD, SC Silverstein: Receptors for C3b and C3bi promote phagocytosis but not the release of toxic oxygen from human phagocytes. *J Exp Med* 1983;158:2016–2023.
- 41 Roubey RA, Ross GD, Merrill JT, Walton F, Reed W, Winchester RJ, Buyon JP: Staurosporine inhibits neutrophil phagocytosis but not iC3b binding mediated by CR3 (CD11b/CD18). *J Immunol* 1991;146:3557–3562.
- 42 Greenberg S, Silverstein SC: Phagocytosis; in Paul WE (ed): *Fundamental Immunology*, ed 3. New York, Raven, 1993, pp 941–964.
- 43 Romani L, Moretti S, Fallarino F, Bozza S, Ruggeri L, Casagrande A, Aversa F, Bistoni F, Velardi A, Garaci E: Jack of all trades: thymosin alpha 1 and its pleiotropy. *Ann NY Acad Sci* 2012;1269:1–6.